

## Study of Variation of R.M.S. Strain with Average Particle Size of Different Phases Evolved During High Energy Ball Milling Of Anatase TiO<sub>2</sub> Suggesting Simultaneous Occurrence of Hall-Petch Effect and Inverse Hall-Petch Effect

Punarbasa Bose<sup>1</sup>

<sup>1</sup> Department of Physics, Hooghly Women's College, Hooghly, West Bengal.

---

**Abstract** Average particle size (Grain size) plays an important role in controlling material strength. In polycrystalline materials with grain sizes in the micrometre range, strength increases with decreasing size obeying Hall–Petch relation. But in polycrystalline solids having average grain sizes of the order of a few nanometers (nm) an opposite behaviour was found, called an inverse Hall–Petch effect (IHPE). The reversal of behavior takes place at a certain critical size at which the strength becomes maximum and is termed as “strongest size”. In the present work simultaneous occurrence of Hall–Petch as well as inverse Hall–Petch effect (IHPE) has been reported. In the polymorphic mixture of different TiO<sub>2</sub> phases, obtained by ball milling of spec. pure anatase TiO<sub>2</sub>, it is found that for anatase TiO<sub>2</sub> phase and rutile TiO<sub>2</sub> phase, variation of r.m.s. strain with particle size is in agreement with Hall-Petch relation whereas an inverse Hall-Petch effect is occurring in case of TiO<sub>2</sub>-II phase simultaneously, solely depending upon whether the saturation particle size of individual phase is above or below the critical particle size or strongest size for that phase. The phases (anatase and rutile) with saturation particle size above 10 nm shows Hall-Petch effect whereas the phase having saturation particle size below 10 nm show an inverse Hall-Petch effect.

**Keywords-** Hall-Petch effect, inverse Hall–Petch effect (IHPE), particle size, r.m.s. strain, strongest size.

---

Date of Submission: 22-02-2018

Date of acceptance: 09-03-2018

---

### I. INTRODUCTION

Average particle size (Grain size) plays an important role in controlling material strength. In polycrystalline materials, i.e., materials with grain sizes in the micrometer range, strength increases with decreasing size. This is known as the Hall–Petch effect [1,2] and was first explained in terms of the piling up of dislocations, created by the shearing of crystal planes in each grain, at the grain boundaries. With the advent of modern nanotechnology it is now possible to synthesize nanocrystalline solids, i.e. polycrystalline solids having average grain sizes of the order of a few nanometers (nm). Due to their unique mechanical properties [3] these materials are now gaining attention of scientific as well as industrial world for improved technological applications. The Hall-Petch law predicts that a nanocrystalline solid should have huge hardness, usually much higher than its usual polycrystalline phase. As the grains become smaller, the effect of dislocation blocking increases, thereby strengthening the material. But with the synthesis of nanocrystals, with grains in the nanometre range, the opposite behavior was found.

Nano crystalline materials show promises for applications in a wide range of fields, particularly because of their high strength-to-weight ratios when compared with their coarse grained counterparts. However, the high strength expected for Nano crystalline materials has been questioned by several investigations, which claimed a decrease in the yield stress ( $\sigma_{yield}$ ) below a critical grain size [4–14]

Classically, one would expect an increase in  $\sigma_{yield}$  for smaller grain sizes according to the Hall–Petch equation [1, 2] given by:

$$\sigma_{yield} = \sigma_o + k_y d^{-1/2} \quad (1)$$

where  $\sigma_o$  is the friction stress in the absence of grain boundaries,  $k_y$  is a constant and  $d$  is the grain size. In other words, the yield stress increases as grain size decreases because pile-ups in fine-grained materials contain fewer dislocations, the stress at the tip of the pile-up decreases and, thus, a larger applied stress is required to generate dislocations in the adjacent grain. In other words, the yield stress increases as grain size decreases. But in very small grains, this mechanism will break down because grains are unable to support dislocation pile-ups. As a consequence, a threshold value is expected at which a maximum yield stress can be achieved. The critical size at which the strength becomes maximum is termed as “strongest size” by Sidney Yip [15]. Typically, this is expected to occur for grain sizes below 10 nm for most metals [16, 17]. An inverse Hall–Petch effect has been

observed for nanocrystalline materials by a large number of researchers. In the present work simultaneous occurrence of Hall–Petch as well as inverse Hall–Petch effect (IHPE) has been reported.

## II. EXPERIMENTAL DETAILS

Nanometric particles can be obtained by several means. High-energy ball milling is one of the conventional methods of mechanical processing for production of nanocrystalline or amorphous materials. Ceramic powder materials (~micron size) processed by high energy ball mill usually undergoes several mechanochemical phase transitions and the final products are composed of different phases along with contaminations from milling media. Several polymorphs of TiO<sub>2</sub> are known to exist namely, anatase (tetragonal; space group, *I41/amd*; density, 3.89), rutile (tetragonal; space group, *P4<sub>2</sub>/mnm*; density, 4.25), brookite (orthorhombic; space group, *Pcab*; density, 4.12), high-pressure phase TiO<sub>2</sub> –II (orthorhombic; space group, *Pbcn*; density, 4.34) and another high-pressure phase TiO<sub>2</sub> (B) (monoclinic; space group, *P2<sub>1</sub>/c*; density, 5.06). Mechanochemical polymorphic transformations of high purity anatase TiO<sub>2</sub> by high energy vibratory ball mill were reported previously [18-20].

A 10g charge of high purity (99.99%) anatase TiO<sub>2</sub> (Aldrich, Milwaukee, WI) was dry milled by SPEX 8000 Mixer mill (Glen Creston Ltd., U.K.) in a high purity  $\alpha$ -Al<sub>2</sub>O<sub>3</sub> vial using only one ball of  $\alpha$ -Al<sub>2</sub>O<sub>3</sub> under sealed atmosphere. X-ray powder diffraction data of unmilled and ball milled samples were collected in step scan mode (step size = 0.02° 2 $\theta$ , counting time = 2s/step) by employing CoK $\alpha$ <sub>1</sub> radiation from a highly stabilized and computer coupled x-ray powder diffractometer (Philips, model PW 1710). A more detailed description of sample preparation and data collection are reported in the earlier papers [18-20].

## III. MICROSTRUCTURE EVOLUTION BY X-RAY DIFFRACTION

Due to several polymorphic transformations and a considerable amount of contamination from grinding media, most of the x-ray diffraction profiles of individual phase in the x-ray powder diffraction pattern of ball milled powder are completely or partially overlapped. A crystal structural model for polycrystalline material namely, the Rietveld method would be the best method for microstructure characterization as well as for quantitative estimations of this type of multiphase material. The LS1 [21] software, a Rietveld's powder structure refinement procedure based on refinement of both the structural and microstructural parameters simultaneously using pseudo-Voigt profile fitting function, has been adopted in the present study. The materials studied in the present case are multiphase. The Rietveld's method [22, 23] was developed to refine a crystal structure from powder diffraction data and is now being successfully applied for quantitative estimations of the individual component of a composite material considering all refined structural parameters of individual phases of a multiphase sample, and the phase concentration (volume/weight fraction) in the mixture [22]. The powder diffraction patterns were simulated with the help of LS1 software [21] providing all necessary structural and instrumental information and some starting values of microstructural parameters of individual phases as. Besides an analytical peak shape function the theoretical modelling also require crystal structure parameters (lattice parameter, temperature factor, fractional coordinates, occupancy, etc) and instrumental parameters (FWHM, peak-asymmetry, Gaussianity of profiles over whole range of 2 $\theta$  to be analyzed) for a standard material without any lattice imperfection. The weight fraction (Wt.%) for individual phases are determined following Lutterotti et. al. [24]. In the present study, a specially prepared Si [25] is taken as the instrumental standard and the most suitable pseudo-Voigt analytical function [26] is adopted for fitting of the experimental profiles. The structure refinement along with size-strain broadening was carried out simultaneously by adopting the standard procedure [21, 27]. Average particle size  $\langle D \rangle$  and r.m.s. strain  $\langle \epsilon^2 \rangle^{1/2}$  values were obtained following the Fourier single-peak analysis [27].

## IV. RESULTS AND DISCUSSION

To analyse a multi-phase sample like the present one the most problem faced is to estimate the volume contents of individual phases as reflections of individual phases are partially or completely overlapped.

All experimental patterns ( $I_o$ ), (i.e. observed x-ray powder diffraction pattern of as-received unmilled (0h) and ball-milled (16, 32, 64 and 100h) TiO<sub>2</sub> powders) are fitted with respective simulated patterns ( $I_c$ ) and shown in Fig.1.

Evolution of different phases of TiO<sub>2</sub> during continuous ball milling of pure anatase TiO<sub>2</sub> and variation of phase content (wt. %) of different phases with increasing milling time are tabulated in Table-1. Evolution of different phases has been discussed in detail in an article by the Bose et.al [18].

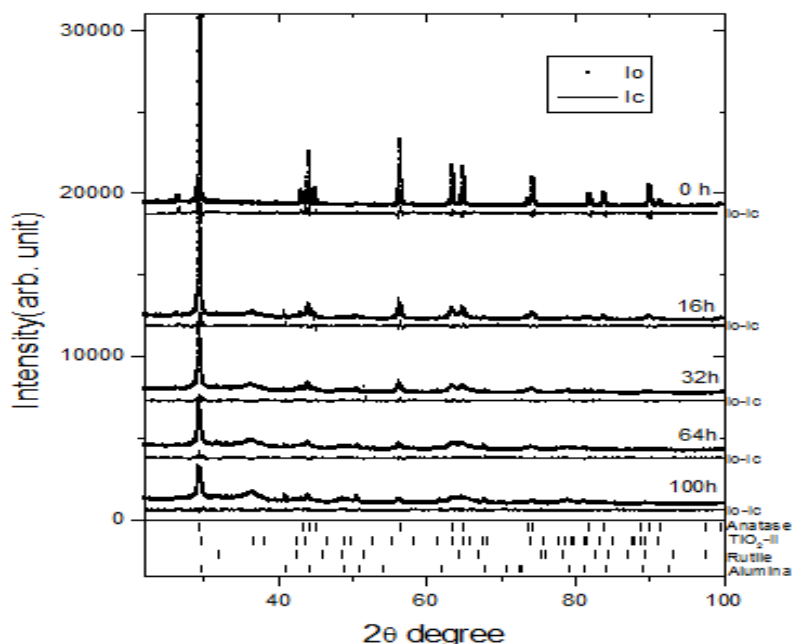


**Figure 1.** Graphical representation of Rietveld analysis for unmilled and milled anatase TiO<sub>2</sub> powder for 16, 32, 64 and 100h: small circles (I<sub>o</sub>) represent experimental data points and line through the circles represent simulated as well as refined profile.

**Table 1. Evolution of different phases of TiO<sub>2</sub> during ball milling of anatase TiO<sub>2</sub> revealed by Rietveld's analysis.**

Milling Time in hour	Phases present in the system (Wt %)			
	Anatase TiO <sub>2</sub>	TiO <sub>2</sub> -II	Rutile TiO <sub>2</sub>	Impurity (α-Al <sub>2</sub> O <sub>3</sub> )
0	100	0	0	0
16	53.1	39	1.1	6.7
32	35	57.6	1.5	4.1
64	24.2	62.9	3.4	7.5
100	16.2	63.9	3.5	13.6

From the nature of variation of phase content (wt. %) of different phases with increasing milling time it is evident that the anatase phase transformed mainly to high pressure TiO<sub>2</sub> –II phase. As the intergrowth of a new phase always leads to release in lattice strain, anatase phase could not transform to TiO<sub>2</sub> –II phase due to insufficient amount of shock energy. This may be the probable explanation of ‘plateau region’ of anatase-TiO<sub>2</sub>-II phase transition. The quantitative estimation also shows that there is a small increment of TiO<sub>2</sub>-II phase in the last stage of ball milling (80-100h) and a corresponding decrease in anatase TiO<sub>2</sub>. It suggests that in this stage of milling, the stored energy again reached the critical value for anatase to TiO<sub>2</sub>-II phase transition and the transformation was further activated in the 4<sup>th</sup> stage of milling. As the wt% of rutile phase increases monotonically even in the last stage of ball milling, the possibility of TiO<sub>2</sub>-II to rutile transformation may not be ruled out [27- 29].

Figures 2(a), 2(b) and 2(c) show the variation of lattice strain with particle size of anatase- TiO<sub>2</sub>, rutile-TiO<sub>2</sub> and TiO<sub>2</sub>-II phase respectively. These values are calculated following single peak analysis (SPA) method [27] incorporated in the Rietveld's powder profile refinement software [21]. Extracted values are shown in Table-2 (a) and Table-2 (b) respectively and plotted in the Figures 2(a), 2(b) and 2(c). In this methods of analysis, particle size and lattice strain (r.m.s.) values are considered isotropic in nature. Particle size of anatase TiO<sub>2</sub> decreases gradually with increasing milling time and reduces to ~35 nm after 40 h as calculated from SPA method. On further milling no significant change in particle size is observed even up to 100h. This is quite similar to earlier observation [17] and also agrees well enough with the observations of Welhem [30-32] and Ren et al. [29] of attaining saturation in particle size due to an equilibrium between breakage and re-welding process occurring simultaneously during a milling process. But in case of high pressure TiO<sub>2</sub>-II phase the particle size remains almost constant (~2.5 nm) throughout the milling process, as if the phase transition prefers this particular particle size. This observation corroborates the finding of Ren et al. [29].

As the intergrowth of a new phase always leads to release in lattice strain, anatase phase could not transform to TiO<sub>2</sub>-II phase due to insufficient amount of shock energy. This may be the probable explanation of ‘plateau region’ of anatase-TiO<sub>2</sub>-II phase transition. The quantitative estimation also shows that there is a small increment of TiO<sub>2</sub>-II phase in the last stage of ball milling (80-100h) and a corresponding decrease in anatase TiO<sub>2</sub>. It suggests that in this stage of milling, the stored energy again reached the critical value for anatase-TiO<sub>2</sub>-II phase transition and the transformation was further activated in the 4<sup>th</sup> stage of milling. As the wt% of rutile phase increases monotonically even in the last stage of ball milling, the possibility of TiO<sub>2</sub>-II to rutile transformation may not be ruled out [28- 30].

The variations of lattice strain with average particle size of different TiO<sub>2</sub> phases at different stages of milling (i.e., 16, 32, 64, 100 hours) are shown in Table 2(a) and Table 2(b) and the same are plotted in Fig. 2(a), 2(b) and 2(c) respectively to demonstrate variation of r.m.s. strain with decreasing average particle size <D>. The scale for average particle size <D> is taken from higher to lower values to demonstrate striking feature of variation of strain with decreasing particle size. The lattice strain of anatase TiO<sub>2</sub> phase and rutile TiO<sub>2</sub> phase increase with decreasing average particle size <D>. But in case of high-pressure TiO<sub>2</sub>-II lattice strain decreases with decreasing particle size as the milling time increases.

**Table-2(a) Variation of particle size and r.m.s. strain of anatase and rutile phases indicating Hall-Petch Effect**

Phases	Milling time (h.)	Particle Size <D> (nm)	r.m.s Strain x 10 <sup>3</sup>
Anatase	0	60.6	1.32
	16	42.7	3.73
	32	38.4	4.45
	64	35.3	5.17
	100	34.4	5.23
Rutile	0	-	-
	16	44.4	0.91
	32	43.4	3.03
	64	42.0	4.98
	100	40.9	5.24

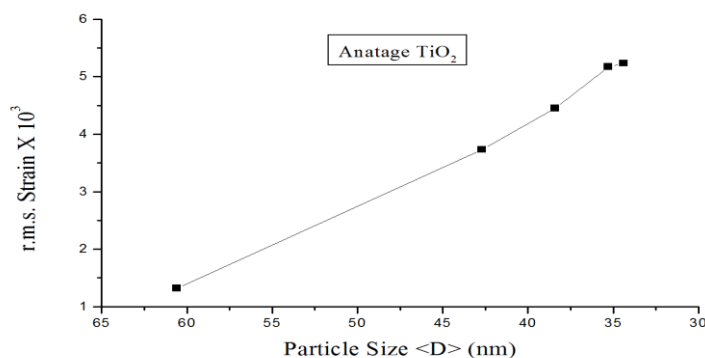


**Figure 2(a) Variation of r.m.s. strain with particle size for anatase-TiO<sub>2</sub>**

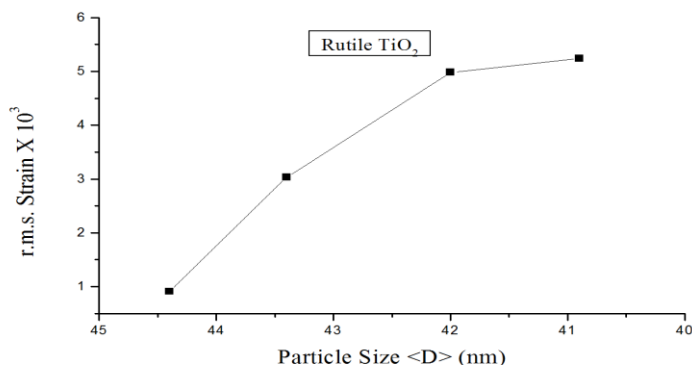


Figure 2(b) Variation of r.m.s. strain with particle size for rutile-TiO<sub>2</sub>

Table- 2(b) Variation of particle size and r.m.s. strain of TiO<sub>2</sub>-II phase indicating Inverse Hall-Petch Effect

Phases	Milling time (h.)	Particle Size <D> (nm)	r.m.s Strain x 10 <sup>3</sup>
TiO <sub>2</sub> -II	0	-	-
	16	2.8	10.15
	32	2.7	8.12
	64	2.6	7.08
	100	2.5	7.05

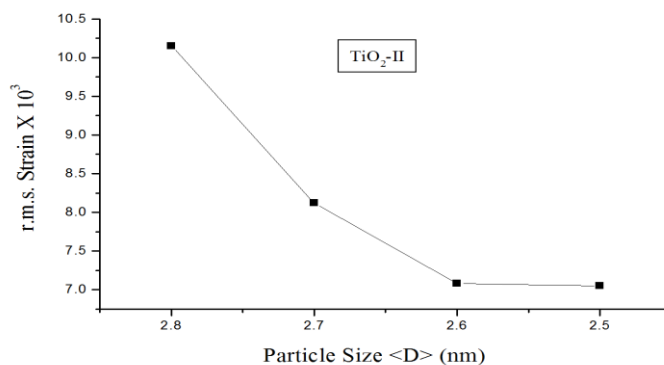


Figure 2(c) Variation of r.m.s. strain with particle size for rutile-TiO<sub>2</sub>-II

As it is evident from Table 2(a) and Fig. 2(a) and Fig. 2(b) that the r.m.s. strain of anatase TiO<sub>2</sub> phase and rutile TiO<sub>2</sub> phase increases with decrease in particle size and this variation in anatase TiO<sub>2</sub> phase and rutile TiO<sub>2</sub> phase is in agreement with Hall-Petch effect. But in case of TiO<sub>2</sub>-II phase strain decreases while particle size also decreases very slowly. This may be explained in the light of inverse Hall- Petch effect (IHPE) where for very small grains, dislocation pile up mechanism will break down because grains are unable to support dislocation pile-ups. For most metals typically, this is expected to occur for grain sizes below 10 nm [14, 15]. Although enough data is not available for such critical size for ceramic substances, but, in the present study it is observed that after 100 hours of milling the particle size of anatase phase reached a saturation value (~15nm) whereas rutile TiO<sub>2</sub> phase assumes the saturation particle size (~16nm). Both the saturation particle size being more than 10 nm. Hence those two phases can with stand pileup of dislocation at grain boundary and causes increase in r.m.s. strain with deceasing particle size. But in case of TiO<sub>2</sub>-II phase the saturation particle size becomes (~2nm) which is much smaller than that of the other two TiO<sub>2</sub> phase (~15nm) and perhaps due to such small grain size there is an onset of IHPE. Thus the dissipation of impact-shock energy due to particle fracture stops and then the accumulated impact energy is chiefly utilized for stress release of highly stressed TiO<sub>2</sub>-II

particles by the process of passage of dislocation to the closely spaced nano-neighbours and annihilation of dislocation there. As a result, the lattice strain of this phase decreased with the decrease of average particle size.

## I. CONCLUSION

In the polymorphic mixture of different TiO<sub>2</sub> phases it is observed that for anatase TiO<sub>2</sub> phase and rutile TiO<sub>2</sub> phase variation of r.m.s. strain with particle size is in agreement with Hall-Petch relation whereas an inverse Hall-Petch effect is occurring simultaneously in case of TiO<sub>2</sub>-II phase solely depending upon whether the saturation particle size of individual phase is above or below the critical particle size or strongest size for that phase, of dimension 10 nm. The phases (anatase and rutile) with saturation particle size above 10 nm shows Hall-Petch effect whereas the phase having saturation particle size below 10 nm shows inverse Hall-Petch effect.

## REFERENCE

- [1]. E.O. Hall, *Proc Phys Soc London B*, 64, 1951; 747.
- [2]. N.J. Petch, *J Iron Steel Inst*, 25, 1953; 174.
- [3]. Meyers MA, Mishra A, Benson DJ, Mechanical properties of nanocrystalline materials. *Progr Mater Sci*, 2006, 51:427-556
- [4]. A.H. Chokski, A. Rosen, J. Karch, H. Gleiter. *Scr Metall* 23, 1989; 1679.
- [5]. G.W. Nieman, J.R. Weertman, R.W. Siegel, *Scr Metall* 23, 1989; 2013.
- [6]. K. Lu, W.D. Wei, J.T. Wang, *Scr Metall Mater*, 24, 1990; 2319.
- [7]. G.W. Nieman, J.R. Weertman, R.W. Siegel, *J Mater Res*, 6, 1991; 1012.
- [8]. G.E. Fougere, J.R. Weertman, R.W. Siegel, S.Kim, *Scr Metall Mater* 26, 1992; 1879.
- [9]. A.M. El-Sherik, U. Erb, G. Palumbo, K.T. Aust, *Scr Mater*, 27, 1992; 1185.
- [10]. V.Y. Gertsman, M. Hofmann, H. Gleiter, R. Dirringer, *Acta Mater*, 42, 1994; 3539.
- [11]. P.G. Sanders, J.A. Eastman, J.R. Weertman, *Acta Mater*, 10, 1997; 4019.
- [12]. C.A. Schuh, T.G. Nieh, T. Yamasaki, *Scr Mater*, 46, 2002; 735.
- [13]. A. Giga, Y. Kimoto, Y. Takigawa, K. Higashi, *Scr Mater*, 55, 2006; 143.
- [14]. S. Yip *Nanocrystals - The strongest size. Nature*, 391, 1998, 532-533
- [15]. T.G. Nieh, J. Wadsworth, *Scr Metall Mater*, 25, 1991; 955.
- [16]. J Eckert, J.C. Holzer, C.E. Krill, W.L. Johnson, *J Mater Res*, 7, 1992; 1751.
- [17]. J. Chaudhuri, M.L. Ram, B.K. Sarkar, *J. Mat. Sc.*, 29, 1994, 3484.
- [18]. S. Sen, M.L. Ram, S. Roy, B.K. Sarkar, *J. Mater. Res.*, 14, 1999, 841.
- [19]. P. Bose, S. K. Pradhan and Suchitra Sen, *Mater. Chem. Phys*, 86, 2003, 73.
- [20]. L. Lutterotti, P. Scardi, P. Maistrelli, *J. Appl. Crystallogr.*, 25, 1992, 459.
- [21]. H.M. Rietveld, *Acta Crystallogr.*, 22, 1967, 151.
- [22]. H.M. Rietveld, *J. Appl. Crystallogr.*, 2, 1967, 65.
- [23]. L. Lutterotti, S.K. Pradhan, S. Gialanella, A.R. Yavari, *Met. Res. Soc. Symp. Proc.*, 1994
- [24]. J.G.M. Van Berkum, *Ph.D. Thesis*, Delft University of Technology, The Netherlands, 1994.
- [25]. R.A. Young, D.B. WILES, *J. Appl. Cryst.*, 15, 1982, 430.
- [26]. A. Benedetti, G. Fagherazzi, S. Enzo, M. Battagliarin, *J. Appl. Cryst.*, 21, 1988, 543.
- [27]. S. Begin-Colin, G. Le caer, A. Mocellin, M. Zandona, *Phil. Mag. Letters.*, 69, 1994, 1.
- [28]. S. Begin-Colin, T. Giroto, G. Le caer, A. Mocellin, *J. Solid State Chem.*, 149, 2000, 41
- [29]. R. Ren, Z. Yang, L.L. Shaw, *J. Mater. Sc.*, 35, 2000, 6015.
- [30]. N.J Welham, *Mater. Sc. & Eng.A.*, 255, 1998, 81.
- [31]. N.J Welham, *J. Mater. Res.*, 13, 1998, 1607.
- [32]. N.J Welham, *J. Mater. Res.*, 14, 1999, 619.

International Journal of Engineering Science Invention (IJESI) is UGC approved Journal with Sl. No. 3822, Journal no. 43302.

Punarbasa Bose "Study of Variation of R.M.S. Strain with Average Particle Size of Different Phases Evolved During High Energy Ball Milling Of Anatage Tio2 Suggesting Simultaneous Occurrence of Hall-Petch Effect and Inverse Hall-Petch Effect "International Journal of Engineering Science Invention (IJESI), vol. 07, no. 03, 2018, pp13-18